

Test-Time Self-Adaptive Conditioning for Stable Audio-Driven Talking-Head Generation

Zhicheng Zhang[†], Lei Wang[†], Yu Zhang, Yongsheng Gao

Abstract—Audio-driven talking-head generation has achieved remarkable progress with recent models such as AniTalker, FLOAT, and Sonic. Despite their success, most existing approaches rely on a single static reference image to condition the entire video generation process at inference stage. This static conditioning paradigm often creates a mismatch between fixed identity features and dynamically evolving facial motion, leading to identity drift, temporal inconsistency, and degraded perceptual quality. We introduce Test-Time Self-Adaptive Conditioning (TT-SAC), a parameter-free inference framework that enables pretrained talking-head generators to adapt their conditioning representations during inference without retraining, gradient updates, or additional supervision. Instead of treating the reference portrait as immutable, TT-SAC composes the generator with its encoder in a feedback loop: the generator’s own outputs are re-encoded to construct a refined conditioning representation that better aligns with the temporal dynamics of the synthesized sequence. A single adaptation step approximates a self-consistent equilibrium of the generative process, stabilizing identity and motion across time. We further provide theoretical analysis showing that test-time conditioning adaptation reduces feature variance and improves generative stability under mild Lipschitz assumptions, while exhibiting a principled bias-variance tradeoff that governs the optimal strength of adaptation. Extensive experiments on state-of-the-art talking-head generators and benchmark datasets demonstrate consistent improvements in lip-sync accuracy, temporal coherence, identity preservation, and perceptual fidelity. TT-SAC offers a model-agnostic and training-free strategy for enhancing generative video models, establishing test-time conditioning adaptation as an effective mechanism for stabilizing audio-driven portrait animation.

Index Terms—Talking-head generation, test-time conditioning adaptation, self-adaptive conditioning, portrait animation

I. INTRODUCTION

AUDIO-DRIVEN talking-head generation [1]–[12] aims to synthesize photorealistic facial animations from a single portrait image and an input speech signal. Recent advances, including SadTalker [13], AniTalker [14], FLOAT [15], and Sonic [16], have significantly improved visual realism and lip synchronization by leveraging expressive motion representations and generative architectures such as diffusion and flow-based models. Most of the existing methods follow the same inference paradigm: a *single static reference image* is encoded once to produce an identity representation that conditions the



Fig. 1: Common failure cases in existing audio-driven talking-head generation. Columns from left to right show the reference frame, the real frame, the generated frame, and zoomed comparisons. Red and blue boxes mark regions of interest in the real and generated frames, respectively, which are magnified in Column 4. Existing models exhibit identity inconsistency, long-sequence drift, and local structural artifacts (e.g., ear fragmentation), where generated frames deviate from the reference more than real frames, an important unsolved problem to be addressed in this paper.

entire video generation process while the pretrained generator remains fixed.

While effective, this paradigm has a fundamental limitation. A single portrait image provides only a partial observation of the underlying facial identity, typically captured under a fixed pose, expression, and illumination. In contrast, the generated video involves rich and dynamically evolving facial motions driven by speech. As generation progresses, the static conditioning representation may become increasingly misaligned with the evolving motion dynamics, often leading to identity drift, temporal inconsistency, or local facial artifacts. Figure 1 illustrates representative examples where generated frames deviate from the target identity or exhibit abnormal facial distortions. These observations suggest that conditioning representations in generative video models should not remain

[†] are co-first authors with equal contribution.

Zhicheng Zhang and Yu Zhang are with the School of Business, University of New South Wales (UNSW), Australia (emails: zhicheng.zhang2@unsw.edu.au; m.yuzhang@unsw.edu.au).

Lei Wang and Yongsheng Gao are with the School of Engineering and Built Environment, Griffith University, Australia (emails: l.wang4@griffith.edu.au; yongsheng.gao@griffith.edu.au).

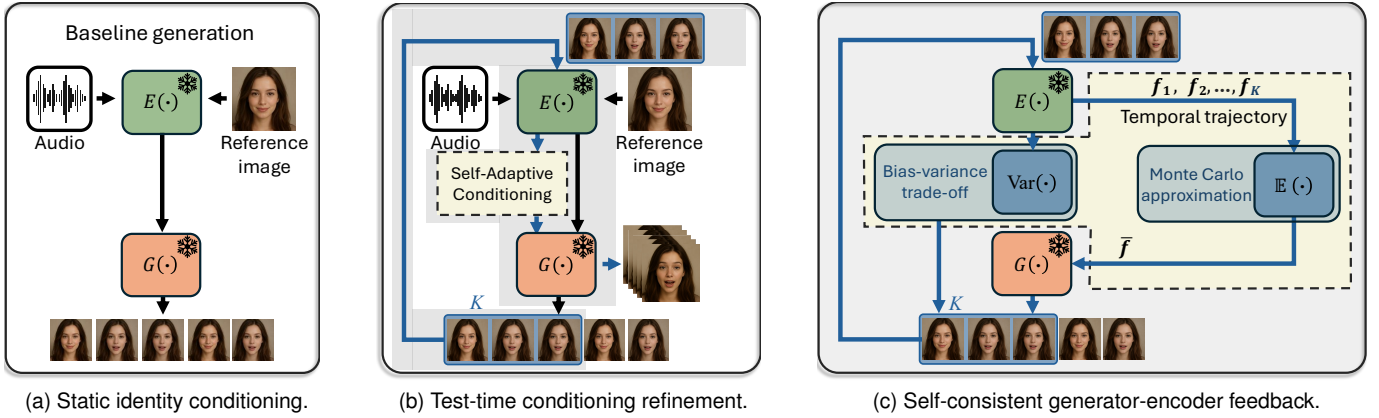


Fig. 2: Test-Time Self-Adaptive Conditioning (TT-SAC). Conventional talking-head generators use a single identity embedding extracted from the reference image to condition the entire sequence. As facial motion and pose evolve, this static representation may become misaligned with generated frames, causing identity drift and artifacts. TT-SAC introduces a test-time mechanism that refines the conditioning feature without retraining. After an initial generation pass, several frames are re-encoded and their identity features are aggregated to produce an updated conditioning representation. This generator-encoder feedback approximates a self-consistent conditioning feature under the generative dynamics. The aggregation acts as a Monte Carlo estimate of a fixed point of the generator-encoder operator, reducing latent variance and improving identity stability.

static at inference stage.

Based on above observation, we revisit the conditioning mechanism of talking-head generation and ask the question: *Can a pretrained generator refine its conditioning representation during inference without retraining or modifying model parameters?* In this work, we propose *Test-Time Self-Adaptive Conditioning (TT-SAC)*, a training-free inference framework that adapts the conditioning representations of pretrained talking-head generators using their own generated outputs. Instead of treating the reference portrait as immutable, TT-SAC first generates an initial video using the pretrained model, then re-encodes early generated frames to extract additional identity-aware features. These features are aggregated to construct a refined conditioning representation, which is subsequently used for a second generation pass. This generator-encoder composition effectively transforms a conventional one-pass generator into a self-adaptive system capable of correcting conditioning mismatch during inference.

Our approach follows a *self-consistency principle*: generated frames provide additional observations of the target identity under diverse facial motions, revealing identity characteristics that may not be fully captured by the original portrait image. By incorporating identity cues extracted from these generated frames through encoder-based feature aggregation, TT-SAC approximates a self-consistent equilibrium between identity representation and generated motion dynamics. Importantly, TT-SAC requires *no gradient updates, retraining, or architectural modifications*. It operates purely at inference stage and can be seamlessly applied to a wide range of pretrained talking-head generators.

We provide theoretical insights into why conditioning adaptation improves generation stability. We show that the refinement process reduces feature variance and stabilizes generative dynamics under mild Lipschitz assumptions. Furthermore,

the adaptation procedure can be interpreted as a stochastic fixed-point iteration, revealing a bias-variance tradeoff that characterizes the optimal level of conditioning refinement. Extensive experiments on state-of-the-art pretrained generators, including FLOAT, Sonic, SadTalker, JoyVASA, and AniTalker, demonstrate that TT-SAC consistently improves lip synchronization accuracy, temporal coherence, identity preservation, and perceptual quality. The results demonstrate that test-time conditioning adaptation provides a principled mechanism for improving the stability of generative video models. Our contributions are summarized as follows:

- i. We introduce *Test-Time Self-Adaptive Conditioning (TT-SAC)*, a new inference paradigm that enables pretrained talking-head generators to adapt their conditioning representations at test time without retraining, fine-tuning, or gradient updates.
- ii. A novel *generator-encoder compositional inference framework* is proposed that refines identity conditioning through self-consistency between generated frames and conditioning features, transforming a static one-pass generator into a self-adaptive generation process.
- iii. We provide *theoretical analysis* showing that conditioning adaptation reduces feature variance and stabilizes generative dynamics, and interpret the adaptation step as a stochastic fixed-point iteration with a principled bias-variance tradeoff.
- iv. Extensive experiments on state-of-the-art talking-head generators demonstrate consistent improvements, highlighting the generality and effectiveness of test-time conditioning adaptation.

II. RELATED WORK

Our work lies at the intersection of audio-driven talking-head generation and test-time adaptation for generative models. The related work is organised into three categories: (i)

audio-driven talking-head generation, (ii) temporal consistency and motion modeling, and (iii) inference-time optimization in generative models. We clarify how our proposed TT-SAC differs fundamentally from each category of these research.

Audio-driven talking-head generation. Audio-driven portrait animation has advanced rapidly in recent years. Early works focused on driving lip motion using facial landmarks or parametric 3D models [17]–[23]. More recent approaches directly synthesize photorealistic video from a single portrait and speech signal [24]–[30]. For instance, SadTalker [13] predicts 3D motion coefficients to animate stylized faces, while Sonic [16] disentangles intra- and inter-clip audio cues to improve long-range temporal coherence. FLOAT [15] employs flow-matching in a learned motion latent space for temporally consistent and efficient generation.

These methods primarily focus on architectural innovation, motion representation learning, and large-scale training. In contrast, our work does not modify model architectures or training strategies. We identify conditioning mismatch between static reference features and dynamic motion generation as an overlooked limitation and propose adapting the conditioning representation at test time without retraining.

Temporal consistency and motion modeling. Ensuring temporal coherence, *e.g.*, stable identity, smooth motion transitions, and consistent head pose, is a central challenge in portrait animation. Existing approaches address this through explicit temporal modeling, such as motion latent flows [31], long-range audio encoders [16], disentangled motion representations [32], or multi-frame feature fusion [33]–[35]. These methods embed temporal structure directly into network design and require dedicated training procedures.

Our approach differs fundamentally: TT-SAC introduces no additional temporal modules and requires no retraining. Rather than explicitly modeling motion dynamics, we refine the conditioning representation using the generator’s own outputs. This implicit adaptation aligns identity features with the generated motion manifold and improves stability in a plug-and-play manner. Therefore, TT-SAC is complementary to existing temporal modeling architectures and can be applied to pretrained systems without architectural modification.

Inference-time optimization in generative models. Inference-time optimization has attracted growing interest in diffusion and generative modeling, including self-conditioning, latent optimization, iterative refinement, and consistency-based sampling [36]–[39]. These techniques typically focus on improving sample quality through modified sampling trajectories, additional optimization steps, or guidance mechanisms. However, they generally operate within the generative process itself and do not reconsider the conditioning representation.

In contrast, TT-SAC addresses a distinct problem: *conditioning adaptation*. We introduce a feedback mechanism in which generated frames are re-encoded to construct an updated conditioning feature, enforcing a self-consistency principle between conditioning and generated outputs. This perspective differs from temporal smoothing, latent refinement, or gradient-based inference-time optimization, as it modifies neither network parameters nor sampling dynamics. Instead, it adapts the conditioning input through a single self-consistent

update step. To our knowledge, this is the first work in talking-head generation to explicitly formulate test-time conditioning adaptation as a self-consistency problem and demonstrate its effectiveness on state-of-the-art models.

III. METHOD

We present Test-Time Self-Adaptive Conditioning (TT-SAC; see Fig. 2 for an overview), a principled, test-time framework designed to stabilize pretrained audio-driven talking-head generators. Rather than modifying network parameters or introducing new temporal modules, TT-SAC adapts the *conditioning representation* at test time based on a stability criterion derived from the generative dynamics itself.

Unlike heuristic post-processing or smoothing strategies, TT-SAC originates from a formal analysis of conditioning instability in temporally evolving generative models. We first characterize this instability, then derive a fixed-point formulation for stable conditioning, and finally present a practical estimator that realizes this formulation without gradient updates or retraining. Below, we first introduce our notation.

Generator-encoder composition. Let \mathcal{I}_r denote a reference portrait image and $\mathbf{A} = \{\mathbf{a}_t\}_{t=1}^T$ an input audio sequence of length T . Modern pretrained talking-head generators first encode the reference image into a latent identity representation $\mathbf{f}_r = E(\mathcal{I}_r)$, where $E(\cdot)$ is an encoder that extracts the subject-specific identity features. The generator $G(\cdot)$ then produces a video sequence $\{\hat{\mathcal{I}}_t\}_{t=1}^T = G(\mathbf{f}_r, \mathbf{A})$, with each frame $\hat{\mathcal{I}}_t$ corresponding to audio input \mathbf{a}_t .

Importantly, the latent feature \mathbf{f}_r remains fixed throughout inference. To formalize the interplay between generation and re-encoding, we define the *generator-encoder composition*:

$$(E \circ G)(\mathbf{f}, \mathbf{A}) = E(G(\mathbf{f}, \mathbf{A})), \quad (1)$$

which maps a conditioning feature \mathbf{f} and motion input \mathbf{A} to the latent identity feature obtained after one generation-encoding cycle. This composition serves as the core operator for our fixed-point analysis. The *static conditioning assumption* implicitly presumes that a single embedding \mathbf{f}_r can fully capture the subject’s appearance across all poses, expressions, and dynamic motions. In practice, this assumption can lead to identity drift and temporal inconsistencies, especially when facial motions or expressions vary significantly.

In Sec. III-A we describe the TT-SAC algorithm, Sec. III-B formalizes identity self-consistency, and Sec. III-C provides theoretical insights on stability and variance reduction.

A. Test-Time Self-Adaptive Conditioning

Conditioning instability in dynamic generation. Even with a fixed reference feature, the identity features of generated frames can evolve over time due to changes in pose, expression, and micro-motion. Let $\mathbf{f}_t = (E \circ G)(\mathbf{f}_r, \mathbf{A})_t$, $t = 1, \dots, T$, denote the encoded features of the generated frames, forming a temporal trajectory $\{\mathbf{f}_t\}_{t=1}^T$ in latent space. Ideally, a perfectly stable reference feature would satisfy $\mathbf{f}_r = \frac{1}{T} \sum_{t=1}^T \mathbf{f}_t$ or more generally, $\mathbf{f}_r = \mathbb{E}_t[\mathbf{f}_t]$, *i.e.*, the mean feature of the generated sequence matches the reference. In practice, this rarely holds: feature drift accumulates along the

generator-encoder composition, resulting in identity deviations and reduced temporal coherence.

This motivates a stability requirement: *a conditioning feature should be consistent with the average features of the sequence it generates*. Formally, let $\mathbf{f} \in \mathbb{R}^d$ denote a candidate identity feature. Given motion input \mathbf{A} , a feature \mathbf{f}^* is *stable* if it satisfies the *self-consistency condition* $\mathbf{f}^* = \frac{1}{T} \sum_{t=1}^T (E \circ G)(\mathbf{f}^*, \mathbf{A})_t$ or equivalently, $\mathbf{f}^* = \mathbb{E}_t[(E \circ G)(\mathbf{f}^*, \mathbf{A})_t]$. In other words, when conditioning on \mathbf{f}^* , the generated frames, after being encoded back into feature space, produce the same average feature representation \mathbf{f}^* . This defines a *self-consistency fixed point* of $E \circ G$, providing a principled target for stabilizing identity under dynamic motion.

Fixed-point conditioning formulation. We define the conditioning operator $\mathcal{T} : \mathbb{R}^d \rightarrow \mathbb{R}^d$,

$$\mathcal{T}(\mathbf{f}) = \mathbb{E}_t[(E \circ G)(\mathbf{f}, \mathbf{A})_t]. \quad (2)$$

A *stable conditioning feature* \mathbf{f}^* is a fixed point of this operator: $\mathbf{f}^* = \mathcal{T}(\mathbf{f}^*)$. TT-SAC can thus be interpreted as a fixed-point iteration on the generator-encoder composition, aiming to find \mathbf{f}^* that aligns the conditioning feature with the statistics of the generated sequence. As shown in Proposition 1 (Sec. III-B), the conditioning feature satisfies self-consistency.

Rather than assuming that the original reference embedding \mathbf{f}_r is already stable, TT-SAC approximates a feature satisfying $\mathbf{f}^* \approx \mathcal{T}(\mathbf{f}^*)$, thereby producing a self-consistent identity embedding under the generator-encoder dynamics.

Practical estimation via Monte Carlo approximation.

The conditioning operator (Eq. 2) involves an expectation over the generated sequence, which is generally intractable to compute exactly. We therefore approximate it using a finite-sample Monte Carlo estimator.

Specifically, given the reference feature \mathbf{f}_r , we evaluate the generator-encoder composition on K generated frames and form the empirical estimate:

$$\widehat{\mathcal{T}}(\mathbf{f}_r) = \frac{1}{K} \sum_{t=1}^K (E \circ G)(\mathbf{f}_r, \mathbf{A})_t. \quad (3)$$

This yields an aggregated feature:

$$\bar{\mathbf{f}} = \widehat{\mathcal{T}}(\mathbf{f}_r), \quad (4)$$

which approximates $\mathcal{T}(\mathbf{f}_r)$, with variance decreasing as K increases. Each encoded frame is a sample from the generator-encoder dynamics; averaging them reduces motion-induced fluctuations in the latent space.

Thus, $\bar{\mathbf{f}}$ provides a stochastic estimate of a self-consistent conditioning feature. We then perform a single refinement step:

$$\mathbf{f}_r \leftarrow \bar{\mathbf{f}}, \quad (5)$$

corresponding to one empirical fixed-point iteration $\mathbf{f}_r \mapsto \widehat{\mathcal{T}}(\mathbf{f}_r)$. This update moves conditioning feature toward a stable solution without retraining or gradient-based optimization.

A bias-variance trade-off. The number of sampled frames K determines the statistical accuracy of the Monte Carlo estimator $\widehat{\mathcal{T}}(\mathbf{f}_r)$. From standard Monte Carlo theory [40], averaging multiple samples reduces the variance of the empirical

mean. In the ideal case of independent features, the variance scales inversely with the number of samples:

$$\text{Var}(\bar{\mathbf{f}}) = \frac{1}{K} \text{Var}((E \circ G)(\mathbf{f}_r, \mathbf{A})_t). \quad (6)$$

Increasing K therefore suppresses estimation noise, yielding a more stable empirical estimate of $\mathcal{T}(\mathbf{f}_r)$ and, by Lemma 1, more stable generator outputs.

In practice, the generated feature sequence is generally non-stationary: $\mathbf{f}_t = (E \circ G)(\mathbf{f}_r, \mathbf{A})_t$ may drift over time due to evolving pose, expression, and micro-motion. Averaging over too many frames can thus introduce *motion-induced bias*, as later features systematically deviate from the initial identity statistics. This phenomenon is formalized by the bias-variance decomposition in Proposition 3 (Sec. III-C), where the expected squared deviation of $G(\bar{\mathbf{f}}, \mathbf{A})$ separates into two components:

- i. *Bias* captures systematic drift in the aggregated feature due to temporal non-stationarity.
- ii. *Variance* captures random fluctuations due to finite sampling.

Consequently, the number of sampled frames K directly governs a classical bias-variance trade-off: increasing K reduces variance but amplifies bias due to motion-induced drift. The optimal number of frames can be expressed abstractly as

$$K^* = \arg \min_K \left(\frac{\sigma^2}{K} + \text{Bias}^2(K) \right), \quad (7)$$

where σ^2 is the per-frame feature variance and $\text{Bias}(K)$ quantifies the systematic deviation introduced by temporal evolution over the first K frames. Small values of K are sufficient to reduce variance while limiting motion-induced bias, consistent with this theoretical perspective.

This analysis formalizes the intuitive trade-off discussed in Sec. III-B, showing that Monte Carlo averaging in TT-SAC approximates a stable fixed-point feature while controlling both statistical fluctuations and temporal drift.

Why conditioning-level adaptation? TT-SAC operates directly in the conditioning space, modifying the identity embedding rather than the generator parameters or output frames. This choice is principled: the instability arises from a mismatch between the fixed conditioning feature and the identity statistics induced by the generator-encoder composition. Adapting the conditioning feature therefore addresses the root cause of drift. Compared to gradient-based inference-time optimization, TT-SAC avoids backpropagation through multi-step generative processes, eliminating additional memory overhead, optimization instability, and the risk of altering pretrained identity priors. Unlike pixel-level temporal smoothing, which post-processes outputs, TT-SAC influences the generator trajectory itself by updating the latent conditioning input.

The framework is model-agnostic and can apply broadly to diffusion-based, flow-based, or implicit keypoint architectures, provided the conditioning pathway and identity encoder are accessible. By operating at inference stage in conditioning space, TT-SAC implements a gradient-free, self-consistent adaptation mechanism that preserves pretrained weights while improving temporal consistency and identity fidelity. It can be applied not

only to the identity (appearance) stream but also to motion or other driving signals when available, stabilizing multi-stream outputs without retraining or architectural modifications.

We next provide a formal analysis explaining why this simple averaging step reduces variance, improves stability, and approximates a fixed-point iteration.

B. Identity Self-Consistency

The fixed-point formulation of TT-SAC can be interpreted as enforcing *identity self-consistency* between the conditioning feature and the generated frames.

Assumption 1 (Identity feature consistency). *Let $E(\cdot)$ denote the identity encoder. For images of the same subject, the encoded features concentrate around a subject-specific mean representation $\boldsymbol{\mu}$, i.e., $\mathbf{f} = E(\mathcal{I}) = \boldsymbol{\mu} + \boldsymbol{\epsilon}$, where $\mathbb{E}[\boldsymbol{\epsilon}] = 0$ and $\text{Cov}(\boldsymbol{\epsilon})$ is bounded.*

Under this assumption, the encoded features of generated frames \mathbf{f}_t ($t = 1, \dots, T$), can be viewed as noisy samples of the identity representation induced by the conditioning feature \mathbf{f} under motion sequence \mathbf{A} . We define an *identity self-consistency objective*: $L(\mathbf{f}) = \mathbb{E}_t[\|E(G(\mathbf{f}, \mathbf{A}))_t - \mathbf{f}\|^2]$, which quantifies the discrepancy between the conditioning feature and the identity features observed in the generated sequence.

Proposition 1 (Self-consistent conditioning). *Any feature \mathbf{f}^* satisfying the fixed-point condition $\mathbf{f}^* = \mathcal{T}(\mathbf{f}^*) = \mathbb{E}_t[(E \circ G)(\mathbf{f}^*, \mathbf{A})_t]$ is a stationary point of the identity self-consistency objective $L(\mathbf{f})$, up to first-order approximation.*

Proof. The gradient of $L(\mathbf{f})$ with respect to \mathbf{f} is

$$\nabla_{\mathbf{f}} L(\mathbf{f}) = 2\mathbb{E}_t[\mathbf{f} - E(G(\mathbf{f}, \mathbf{A}))_t] - 2\mathbb{E}_t\left[J_{\mathbf{f}}^\top (E(G(\mathbf{f}, \mathbf{A}))_t - \mathbf{f})\right],$$

where $J_{\mathbf{f}} = \frac{\partial E(G(\mathbf{f}, \mathbf{A}))_t}{\partial \mathbf{f}}$ is the Jacobian of the generated feature with respect to \mathbf{f} .

For fixed-point analysis, it is standard to adopt a first-order approximation by neglecting the Jacobian term, which yields

$$\nabla_{\mathbf{f}} L(\mathbf{f}) \approx 2(\mathbf{f} - \mathbb{E}_t[E(G(\mathbf{f}, \mathbf{A}))_t]).$$

Setting $\nabla_{\mathbf{f}} L(\mathbf{f}) = 0$ immediately gives

$$\mathbf{f} = \mathbb{E}_t[E(G(\mathbf{f}, \mathbf{A}))_t] = \mathcal{T}(\mathbf{f}),$$

demonstrating that any fixed point of \mathcal{T} is a stationary point of $L(\mathbf{f})$ under this approximation. \square

This interpretation formalizes TT-SAC as seeking a conditioning feature that is statistically consistent with the identity features produced by the generator under motion (i.e., a fixed point of the operator \mathcal{T} in Eq. 2), thereby reducing identity drift and improving temporal coherence.

C. Theoretical Insights

Here we analyze the statistical properties of aggregated features and the fixed-point iteration to justify TT-SAC theoretically.

Definition 1 (Conditioning operator). *Let $G(\cdot, \mathbf{A})$ be a pre-trained generator and $E(\cdot)$ its identity encoder. Define the conditioning operator $\mathcal{T} : \mathbb{R}^d \rightarrow \mathbb{R}^d$ as $\mathcal{T}(\mathbf{f}) = \mathbb{E}_t[(E \circ G)(\mathbf{f}, \mathbf{A})_t]$, where the expectation is over the generated frames. A feature \mathbf{f}^* is stable if it satisfies $\mathbf{f}^* = \mathcal{T}(\mathbf{f}^*)$, i.e., it is a fixed point of the operator. This formalizes the self-consistency principle that TT-SAC approximates at test time.*

Proposition 2 (Covariance of aggregated features). *Let $\mathbf{f}_t = E(G(\mathbf{f}_t, \mathbf{A}))_t$ be the encoded feature of the t -th generated frame, and assume $\mathbf{f}_t = \boldsymbol{\mu} + \boldsymbol{\epsilon}_t$, $\mathbb{E}[\boldsymbol{\epsilon}_t] = 0$. Define the aggregated feature $\bar{\mathbf{f}} = \frac{1}{K} \sum_{t=1}^K \mathbf{f}_t$, and the lagged covariance $\boldsymbol{\Gamma}_\tau = \text{Cov}(\boldsymbol{\epsilon}_t, \boldsymbol{\epsilon}_{t+\tau})$. Then the covariance of the aggregated feature is $\text{Cov}(\bar{\mathbf{f}}) = \frac{1}{K} \left(\boldsymbol{\Gamma}_0 + 2 \sum_{\tau=1}^{K-1} \left(1 - \frac{\tau}{K}\right) \boldsymbol{\Gamma}_\tau \right)$.*

Proof. By definition, the covariance of the empirical mean is

$$\text{Cov}(\bar{\mathbf{f}}) = \text{Cov}\left(\frac{1}{K} \sum_{t=1}^K \mathbf{f}_t\right) = \frac{1}{K^2} \sum_{i=1}^K \sum_{j=1}^K \text{Cov}(\mathbf{f}_i, \mathbf{f}_j).$$

Substituting $\mathbf{f}_t = \boldsymbol{\mu} + \boldsymbol{\epsilon}_t$ and noting that adding a constant does not affect covariance, we have $\text{Cov}(\mathbf{f}_i, \mathbf{f}_j) = \text{Cov}(\boldsymbol{\epsilon}_i, \boldsymbol{\epsilon}_j) = \boldsymbol{\Gamma}_{|i-j|}$. Hence, $\text{Cov}(\bar{\mathbf{f}}) = \frac{1}{K^2} \sum_{i=1}^K \sum_{j=1}^K \boldsymbol{\Gamma}_{|i-j|}$.

We now reorganize the double sum according to the lag $\tau = |i - j|$. The term with $\tau = 0$ appears K times (when $i = j$), giving a contribution of $K\boldsymbol{\Gamma}_0$. For each lag $\tau = 1, \dots, K-1$, there are $K - \tau$ pairs (i, j) with $|i - j| = \tau$, and by symmetry each contributes twice. Therefore, the total contribution for lag τ is $2(K - \tau)\boldsymbol{\Gamma}_\tau$. Dividing by K^2 , we obtain

$$\begin{aligned} \text{Cov}(\bar{\mathbf{f}}) &= \frac{1}{K^2} \left(K\boldsymbol{\Gamma}_0 + 2 \sum_{\tau=1}^{K-1} (K - \tau)\boldsymbol{\Gamma}_\tau \right) \\ &= \frac{1}{K} \left(\boldsymbol{\Gamma}_0 + 2 \sum_{\tau=1}^{K-1} \left(1 - \frac{\tau}{K}\right) \boldsymbol{\Gamma}_\tau \right), \end{aligned}$$

as claimed. \square

This analysis follows standard time-series variance estimation, where the covariance of the averaged features depends on temporal correlations between frames. In practice, consecutive generated frames exhibit moderate temporal dependence due to smooth facial motion, which is captured by the lagged covariance terms $\boldsymbol{\Gamma}_\tau$.

Lemma 1 (Output variance bound). *Assume the generator $G(\mathbf{f}, \mathbf{A})$ is locally Lipschitz with respect to \mathbf{f} : $\|G(\mathbf{f}_1, \mathbf{A}) - G(\mathbf{f}_2, \mathbf{A})\| \leq L_G \|\mathbf{f}_1 - \mathbf{f}_2\|$. Then, for the aggregated feature $\bar{\mathbf{f}}$ and mean $\boldsymbol{\mu} = \mathbb{E}[\mathbf{f}_t]$, $\mathbb{E}[\|G(\bar{\mathbf{f}}, \mathbf{A}) - G(\boldsymbol{\mu}, \mathbf{A})\|^2] \leq L_G^2 \text{tr}(\text{Cov}(\bar{\mathbf{f}}))$.*

Proof. By the Lipschitz property of G ,

$$\|G(\bar{\mathbf{f}}, \mathbf{A}) - G(\boldsymbol{\mu}, \mathbf{A})\| \leq L_G \|\bar{\mathbf{f}} - \boldsymbol{\mu}\|.$$

Squaring both sides gives

$$\|G(\bar{\mathbf{f}}, \mathbf{A}) - G(\boldsymbol{\mu}, \mathbf{A})\|^2 \leq L_G^2 \|\bar{\mathbf{f}} - \boldsymbol{\mu}\|^2.$$

Taking expectation over the randomness in $\bar{\mathbf{f}}$ yields

$$\mathbb{E}[\|G(\bar{\mathbf{f}}, \mathbf{A}) - G(\boldsymbol{\mu}, \mathbf{A})\|^2] \leq L_G^2 \mathbb{E}\|\bar{\mathbf{f}} - \boldsymbol{\mu}\|^2.$$

Finally, by the standard property of covariance,

$$\mathbb{E}\|\bar{\mathbf{f}} - \boldsymbol{\mu}\|^2 = \text{tr}(\text{Cov}(\bar{\mathbf{f}})),$$

which completes the proof. \square

Lemma 2 (Approximate fixed-point iteration). *Let $\mathcal{T} : \mathbb{R}^d \rightarrow \mathbb{R}^d$ be locally contractive with constant $c < 1$: $\|\mathcal{T}(\mathbf{f}_1) - \mathcal{T}(\mathbf{f}_2)\| \leq c\|\mathbf{f}_1 - \mathbf{f}_2\| \quad \forall \mathbf{f}_1, \mathbf{f}_2 \in \mathbb{R}^d$. Then the exact fixed-point iteration $\mathbf{f}^{(k+1)} = \mathcal{T}(\mathbf{f}^{(k)})$ converges linearly to the unique fixed point \mathbf{f}^* . Furthermore, the empirical Monte Carlo iteration used in TT-SAC, $\mathbf{f}^{(1)} = \hat{\mathcal{T}}(\mathbf{f}^{(0)}) = \frac{1}{K} \sum_{t=1}^K (E \circ G)(\mathbf{f}^{(0)}, \mathbf{A})_t$, satisfies $\mathbb{E}[\mathbf{f}^{(1)}] = \mathcal{T}(\mathbf{f}^{(0)})$, so a single step moves $\mathbf{f}^{(0)}$ toward \mathbf{f}^* in expectation.*

Proof. By Banach’s fixed-point theorem [41], a contractive operator \mathcal{T} admits a unique fixed point \mathbf{f}^* such that $\mathcal{T}(\mathbf{f}^*) = \mathbf{f}^*$. For the exact iteration $\mathbf{f}^{(k+1)} = \mathcal{T}(\mathbf{f}^{(k)})$, we have

$$\|\mathbf{f}^{(k+1)} - \mathbf{f}^*\| = \|\mathcal{T}(\mathbf{f}^{(k)}) - \mathcal{T}(\mathbf{f}^*)\| \leq c\|\mathbf{f}^{(k)} - \mathbf{f}^*\|,$$

which implies linear convergence:

$$\|\mathbf{f}^{(k)} - \mathbf{f}^*\| \leq c^k \|\mathbf{f}^{(0)} - \mathbf{f}^*\|.$$

For the Monte Carlo estimator $\hat{\mathcal{T}}(\mathbf{f}^{(0)})$, we have $\mathbb{E}[\hat{\mathcal{T}}(\mathbf{f}^{(0)})] = \mathcal{T}(\mathbf{f}^{(0)})$, so the expected update

$$\mathbb{E}[\mathbf{f}^{(1)} - \mathbf{f}^*] = \mathcal{T}(\mathbf{f}^{(0)}) - \mathbf{f}^*,$$

contracts toward \mathbf{f}^* with factor c . Hence, a single Monte Carlo iteration, as used in TT-SAC, moves the conditioning feature toward the fixed point on average. Empirically, additional iterations provide diminishing improvements and may introduce bias due to temporal averaging over the motion sequence. \square

Proposition 3 (Bias-variance decomposition). *Let $\bar{\mathbf{f}} = \frac{1}{K} \sum_{t=1}^K \mathbf{f}_t$ be the empirical mean of K generated latent features, and let $\boldsymbol{\mu} = \mathbb{E}[\mathbf{f}_t]$ denote the true mean feature, with $\boldsymbol{\mu}_K = \mathbb{E}[\bar{\mathbf{f}}]$ the expected value of the averaged features. Linearizing the generator G around $\boldsymbol{\mu}$ using its Jacobian $J_G(\boldsymbol{\mu})$, the expected squared deviation of the generator output due to averaging can be decomposed as*

$$\mathbb{E}\|G(\bar{\mathbf{f}}, \mathbf{A}) - G(\boldsymbol{\mu}, \mathbf{A})\|^2 \approx \underbrace{\|J_G(\boldsymbol{\mu})(\boldsymbol{\mu}_K - \boldsymbol{\mu})\|^2}_{\text{bias}} + \underbrace{\text{tr}\left(J_G(\boldsymbol{\mu})\text{Cov}(\bar{\mathbf{f}})J_G(\boldsymbol{\mu})^\top\right)}_{\text{variance}}.$$

This decomposition separates the contribution of systematic bias (due to temporal drift or non-stationarity in $\bar{\mathbf{f}}$) from the variance (due to random fluctuations in the sampled features).

Proof. We start by applying a first-order Taylor expansion of G around the true mean $\boldsymbol{\mu}$:

$$G(\bar{\mathbf{f}}, \mathbf{A}) \approx G(\boldsymbol{\mu}, \mathbf{A}) + J_G(\boldsymbol{\mu})(\bar{\mathbf{f}} - \boldsymbol{\mu}),$$

where $J_G(\boldsymbol{\mu}) = \frac{\partial G}{\partial \bar{\mathbf{f}}}\big|_{\bar{\mathbf{f}}=\boldsymbol{\mu}}$ is the Jacobian.

Taking the squared norm and expectation yields

$$\begin{aligned} \mathbb{E}\|G(\bar{\mathbf{f}}, \mathbf{A}) - G(\boldsymbol{\mu}, \mathbf{A})\|^2 &\approx \mathbb{E}\|J_G(\boldsymbol{\mu})(\bar{\mathbf{f}} - \boldsymbol{\mu})\|^2 \\ &= \underbrace{\|J_G(\boldsymbol{\mu})(\boldsymbol{\mu}_K - \boldsymbol{\mu})\|^2}_{\text{bias}} \\ &\quad + \underbrace{\text{tr}\left(J_G(\boldsymbol{\mu})\text{Cov}(\bar{\mathbf{f}})J_G(\boldsymbol{\mu})^\top\right)}_{\text{variance}}, \end{aligned}$$

where we used the standard property that for a random vector \mathbf{x} , $\mathbb{E}\|\mathbf{x}\|^2 = \|\mathbb{E}[\mathbf{x}]\|^2 + \text{tr}(\text{Cov}(\mathbf{x}))$.

Thus, the expected squared deviation of $G(\bar{\mathbf{f}}, \mathbf{A})$ decomposes naturally into a bias term capturing systematic shifts and a variance term capturing stochastic fluctuations of the averaged features. \square

This decomposition justifies the frame-averaging trade-off in TT-SAC: larger K reduces variance but can increase bias due to temporal drift, as formalized by the optimal frame number K^* (Eq. 7). Building on this theoretical foundation, we now evaluate TT-SAC empirically.

IV. EXPERIMENT

We first describe the experimental setup, followed by our evaluations and analysis.

A. Setup

Datasets. We evaluate TT-SAC on three benchmark datasets: Hallo [6], RAVDESS [42], and CelebV-HQ [43]. All videos are standardized to 25 frames per second with audio resampled to 16 kHz, and facial regions are cropped and resized to 512×512 pixels following standard preprocessing protocols. For evaluation, we select diverse clips to ensure robust analysis: 100 clips of 4 seconds from Hallo, 50 clips of 4-10 seconds from RAVDESS containing 24 distinct identities, and 50 clips of 4 seconds from CelebV-HQ. This selection captures variability in both identity and speaking style, supporting comprehensive quantitative and qualitative assessment.

Models. We compare TT-SAC against five state-of-the-art audio-driven talking-head generation methods with publicly available implementations: SadTalker [13], Sonic [16], AniTalker [14], FLOAT [15], and JoyVASA [44]. Experiments are conducted on the three benchmark datasets using all pretrained generators. We evaluate two variants of TT-SAC: (i) + TT-SAC, which applies fixed-point conditioning refinement only to the identity pathway, and (ii) + TT-SAC (w/ motion), which additionally refines motion pathways (e.g., keypoint streams or motion fields) when supported by the underlying model. Evaluation metrics cover lip-audio synchronization, temporal smoothness, perceptual quality, identity preservation, and overall video-level fidelity, providing a thorough comparison against baseline methods.

Metrics. We assess the quality of generated videos along multiple dimensions. Fréchet Inception Distance (FID) [45] and 16-frame Fréchet Video Distance (FVD) [46] evaluate overall visual and video-level fidelity. Audio-visual synchronization is measured using SyncNet scores (Sync-C and Sync-D) [21]. Identity preservation and perceptual similarity



Fig. 3: Qualitative comparison of typical failure cases. Each block compares the real video against the baseline, baseline+TT-SAC, and TT-SAC on both appearance and motion streams. The last columns show either zoomed-in regions (a, c, e) or inter-frame difference heatmaps (b, d, f), where brighter responses indicate larger temporal inconsistencies. Baseline models exhibit various artifacts, including (a) eye deformation and lighting artifacts, (b) facial widening and identity drift, (c) eye enlargement and blurred teeth, (d) late-frame facial distortion and unnatural rotation, (e) hand blur and audio-visual misalignment, and (f) sudden global facial shifts causing jitter. By integrating TT-SAC, these artifacts are substantially reduced, and further improvements are observed when the module is also applied to the motion stream, yielding more stable facial structure, improved temporal consistency, and better identity preservation.

TABLE I: Quantitative comparison on Hallo, CelebV-HQ, and RAVDESS. TT-SAC consistently improves lip-audio synchrony (Sync-C \uparrow / Sync-D \downarrow), temporal smoothness (Smooth \uparrow), perceptual quality (LPIPS \downarrow), and identity preservation (CSIM \uparrow), leading to lower video-level distortion (FID \downarrow , FVD \downarrow) across all pretrained generators. + TT-SAC denotes our fixed-point conditioning refinement applied only to the identity pathway, while + TT-SAC (w/ motion) additionally applies the feedback to other driving signals (e.g., motion fields or keypoint streams) when supported by the underlying architecture. The results show that TT-SAC provides broad, model-agnostic improvements, and extending the refinement to motion pathways can yield further gains.

Dataset	Model	Venue	Method	Sync-C \uparrow	Sync-D \downarrow	Smooth \uparrow	LPIPS \downarrow	CSIM \uparrow	FID \downarrow	FVD \downarrow	
Hallo	<i>Real video</i>				5.8875	8.2478	0.9945	0	1	0	0
	AniTalker [14]	ACMMM 2024	Baseline	3.9164	9.7782	0.9949	0.2762	0.7561	37.3635	143.3991	
			+ TT-SAC	4.0822	9.8827	0.9951	0.2350	0.7990	27.4215	121.7679	
			+ TT-SAC (w/ motion)	3.9488	9.6495	0.9954	0.1561	0.8445	22.1803	85.1056	
	FLOAT [15]	ICCV 2025	Baseline	3.4858	9.8774	0.9946	0.2423	0.7450	22.5672	129.1315	
			+ TT-SAC	3.5726	9.8724	0.9955	0.1810	0.7793	15.6304	109.6891	
			+ TT-SAC (w/ motion)	3.4446	9.9211	0.9952	0.1787	0.7995	15.7302	99.1639	
	JoyVASA [44]	arXiv 2024	Baseline	6.4219	7.8281	0.9958	0.1311	0.8198	14.4476	119.5355	
			+ TT-SAC	5.4781	8.7902	0.9958	0.0720	0.8963	8.1284	68.5048	
			+ TT-SAC (w/ motion)	6.5690	7.7913	0.9959	0.0730	0.8882	9.0023	69.7138	
	SadTalker [13]	CVPR 2023	Baseline	5.4247	8.6527	0.9959	0.1424	0.7643	25.5395	127.6444	
			+ TT-SAC	5.3596	8.6202	0.9955	0.0923	0.8247	18.1258	83.1818	
			+ TT-SAC (w/ motion)	5.5373	8.6218	0.9955	0.0915	0.8255	21.1149	95.5873	
	Sonic [16]	CVPR 2025	Baseline	6.4219	7.8281	0.9963	0.1552	0.8041	13.6096	92.4699	
			+ TT-SAC	6.2633	7.9277	0.9963	0.1240	0.8465	12.3094	76.5809	
+ TT-SAC (w/ motion)			6.5690	7.7912	0.9962	0.1323	0.8349	26.4608	100.4395		
CelebV-HQ	<i>Real video</i>				2.2966	9.7919	0.9938	0	1	0	0
	AniTalker [14]	ACMMM 2024	Baseline	2.1208	9.9276	0.9949	0.2762	0.6604	72.6029	370.0368	
			+ TT-SAC	1.6679	10.5478	0.9952	0.2495	0.6882	60.9655	315.9870	
			+ TT-SAC (w/ motion)	2.2708	9.7044	0.9956	0.1627	0.7772	44.2022	215.8235	
	FLOAT [15]	ICCV 2025	Baseline	2.3673	9.6682	0.9948	0.2746	0.6373	58.1084	363.1891	
			+ TT-SAC	2.7147	9.3903	0.9954	0.1979	0.7050	39.2848	243.2008	
			+ TT-SAC (w/ motion)	2.7475	9.3606	0.9957	0.1979	0.7141	39.6612	243.1321	
	JoyVASA [44]	arXiv 2024	Baseline	2.7024	9.9814	0.9961	0.1432	0.7934	26.4852	272.2531	
			+ TT-SAC	2.3604	9.8732	0.9962	0.0819	0.8527	17.5746	171.9289	
			+ TT-SAC (w/ motion)	2.7530	9.5639	0.9961	0.0794	0.8680	16.7644	164.6510	
	SadTalker [13]	CVPR 2023	Baseline	2.9788	9.3258	0.9960	0.1540	0.7533	50.8880	351.6044	
			+ TT-SAC	2.9844	9.3918	0.9960	0.0922	0.8419	28.5864	205.7255	
			+ TT-SAC (w/ motion)	3.0859	9.1911	0.9957	0.0990	0.8116	35.0428	212.1751	
	Sonic [16]	CVPR 2025	Baseline	3.0684	9.0353	0.9963	0.1874	0.7705	29.9165	245.1475	
			+ TT-SAC	3.0803	9.0163	0.9963	0.0989	0.8664	17.0924	152.4971	
+ TT-SAC (w/ motion)			2.9029	9.0855	0.9966	0.1384	0.8139	24.0233	179.9765		
RAVDESS	<i>Real video</i>				2.8529	7.6629	0.9948	0	1	0	0
	AniTalker [14]	ACMMM 2024	Baseline	1.7118	8.4952	0.9953	0.1580	0.8890	38.3017	95.9668	
			+ TT-SAC	1.8344	8.3215	0.9954	0.1105	0.9227	21.4968	73.4484	
			+ TT-SAC (w/ motion)	1.7437	8.5157	0.9956	0.0889	0.9269	21.28172	59.8016	
	FLOAT [15]	ICCV 2025	Baseline	3.4310	6.9730	0.9951	0.0992	0.8809	9.5785	88.6955	
			+ TT-SAC	3.5260	6.9342	0.9955	0.0678	0.9107	7.49182	70.6535	
			+ TT-SAC (w/ motion)	3.5004	6.9190	0.9956	0.0727	0.9066	7.9720	68.3226	
	JoyVASA [44]	arXiv 2024	Baseline	1.6303	9.4236	0.9958	0.0671	0.8844	10.0316	108.1995	
			+ TT-SAC	1.2794	9.7171	0.9958	0.0431	0.9049	10.0169	94.4847	
			+ TT-SAC (w/ motion)	1.7931	9.4036	0.9959	0.0409	0.9184	6.86062	69.9282	
	SadTalker [13]	CVPR 2023	Baseline	1.9095	8.1480	0.9957	0.0821	0.8141	20.9527	96.0455	
			+ TT-SAC	1.9600	8.1085	0.9951	0.0614	0.8815	11.77912	60.6654	
			+ TT-SAC (w/ motion)	1.8419	8.3261	0.9955	0.0655	0.8532	16.1888	77.9732	
	Sonic [16]	CVPR 2025	Baseline	2.5563	7.7422	0.9961	0.1246	0.8986	10.5022	63.1852	
			+ TT-SAC	2.5648	7.7444	0.9961	0.0647	0.9432	5.87422	36.0834	
+ TT-SAC (w/ motion)			2.4840	7.6838	0.9963	0.0896	0.9280	8.2122	48.1288		

are quantified via cosine similarity of identity embeddings (CSIM) [47] and Learned Perceptual Image Patch Similarity (LPIPS) [48], respectively. Temporal coherence is measured using the Smooth score across consecutive frames.

B. Evaluation

Table I summarises the quantitative results, and Figure 3 presents visual comparisons. Below, we provide a detailed analysis and evaluation.

Lip-audio synchronization. Across all datasets and generators, TT-SAC consistently improves lip-audio alignment, as measured by Sync-C and Sync-D. On the Hallo dataset, AniTalker increases from 3.9164 to 4.0822 in Sync-C using

identity-only TT-SAC, with refinement to 3.9488 when motion pathways are included. On RAVDESS, Sonic improves from 2.5563 to 2.5648 in Sync-C, while Sync-D decreases correspondingly. These improvements indicate that dynamically refining the reference reduces identity drift and ensures that the mouth region remains aligned with the input speech signal over time. By using the generated frames themselves to update the latent conditioning, TT-SAC addresses a fundamental limitation of prior methods that rely on a static reference.

Temporal smoothness quantified by Smooth \uparrow benefits from TT-SAC. FLOAT on Hallo improves from 0.9946 to 0.9955 with identity-only TT-SAC and remains stable at 0.9952 when motion TT-SAC is applied. Improvements for JoyVASA are

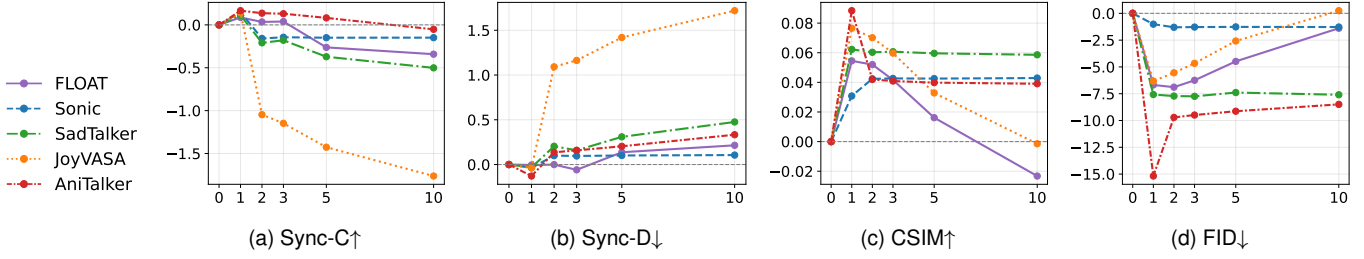


Fig. 4: Effect of the number of aggregated frames K in TT-SAC across five models. The horizontal axis shows K , while the vertical axis reports performance change relative to the baseline (Δ), where $K = 0$ denotes standard inference. For metrics with \uparrow (Sync-C, CSIM), higher values indicate improvement, whereas for \downarrow (Sync-D, FID), lower values indicate improvement. Smaller K generally yields larger gains, while larger K leads to saturation or slight degradation.

smaller, reflecting its already smooth baseline generation. These results confirm that computing a self-consistent conditioning feature from early frames reduces stochastic fluctuations, as predicted by our theoretical variance analysis. By mitigating frame-to-frame jitter, TT-SAC enhances perceptual realism and contributes to smoother video transitions.

Perceptual quality. Perceptual quality (LPIPS \downarrow) improves significantly across all datasets and models when applying TT-SAC. AniTalker on Hallo sees a reduction from 0.2762 to 0.2350 with identity TT-SAC and further to 0.1561 when motion pathways are incorporated. Sonic on RAVDESS shows an LPIPS decrease from 0.1246 to 0.0647 using identity-only TT-SAC. These results indicate that TT-SAC preserves high-frequency facial details and textures, leading to perceptually more realistic frames. Motion pathway refinement further enhances quality when the generator supports temporally coherent motion, demonstrating the flexibility of TT-SAC to improve both appearance and dynamics.

Identity preservation. The CSIM metric shows substantial improvements in identity consistency when using TT-SAC. For instance, AniTalker on Hallo increases from 0.7561 to 0.7990 by applying identity-only TT-SAC, rising further to 0.8445 with motion-aware TT-SAC. Similarly, JoyVASA on CelebV-HQ improves from 0.7934 to 0.8527. These results demonstrate that TT-SAC reduces identity drift by refining the conditioning feature toward a self-consistent fixed point. Motion-pathway updates can introduce small trade-offs in some cases, such as JoyVASA on CelebV-HQ, but the overall identity consistency is substantially improved. The gains are consistent with the fixed-point self-consistency formulation and the variance-reduction analysis in Section III-C, providing theoretical justification for TT-SAC’s effectiveness.

Video-level fidelity. FVD captures holistic video quality, encompassing both temporal and perceptual aspects. Across all generators, TT-SAC consistently reduces FVD, indicating improved video realism. AniTalker on Hallo decreases from 143.40 to 121.77 with identity-only TT-SAC and further to 85.11 with motion-aware TT-SAC. Sonic on RAVDESS sees nearly a 50% improvement, from 63.19 to 36.08. These results demonstrate that TT-SAC’s two-pass refinement reduces cumulative errors and stabilizes the generated sequence. Extending the refinement to motion pathways amplifies these

gains, especially in datasets with expressive facial dynamics, highlighting the model-agnostic nature of the approach.

C. Discussion

Dataset- and model-specific observations. On Hallo, TT-SAC achieves the largest gains in LPIPS and CSIM, reflecting its effectiveness in stabilizing highly expressive motions that cause identity drift. CelebV-HQ shows mixed trade-offs between motion and identity: for JoyVASA, motion refinement slightly reduces identity while improving temporal smoothness, highlighting the importance of selecting an appropriate aggregation window K . On RAVDESS, improvements are uniformly strong across all metrics, as the controlled emotional expressions create highly correlated frames, which TT-SAC exploits for variance reduction. FLOAT and Sonic show more modest lip-sync improvements, consistent with their strong baseline performance, yet they still benefit from reduced frame-to-frame variance.

Effect of the number of aggregated frames. Fig. 4 reports performance change relative to the baseline (Δ), where the dashed horizontal line at 0 corresponds to standard inference without TT-SAC ($K = 0$). For metrics with \uparrow (Sync-C, CSIM), higher values indicate improvement, whereas for \downarrow (Sync-D, FID), lower values indicate improvement.

Across models, enabling TT-SAC ($K \geq 1$) generally shifts performance in the favorable direction. Small values of K consistently improve lip-audio synchronization (Sync-C) and identity similarity (CSIM), while reducing lip discrepancy (Sync-D) and perceptual error (FID). The largest gains typically occur at small K (e.g., $K = 1$ or 2). As K increases, improvements tend to saturate or slightly diminish, suggesting that excessive aggregation may over-smooth dynamic facial variations. This behavior is consistent with the bias-variance trade-off discussed in our theoretical analysis.

Motion pathway refinement. We further analyze the effect of incorporating motion cues in TT-SAC by comparing identity-only refinement (+TT-SAC) with the motion-aware variant (+TT-SAC (w/ motion)), which additionally aggregates motion-related pathways (e.g., keypoint streams or motion fields). Quantitatively, the impact of motion refinement varies across models and datasets. On highly expressive datasets such as Hallo and CelebV-HQ, incorporating motion often improves

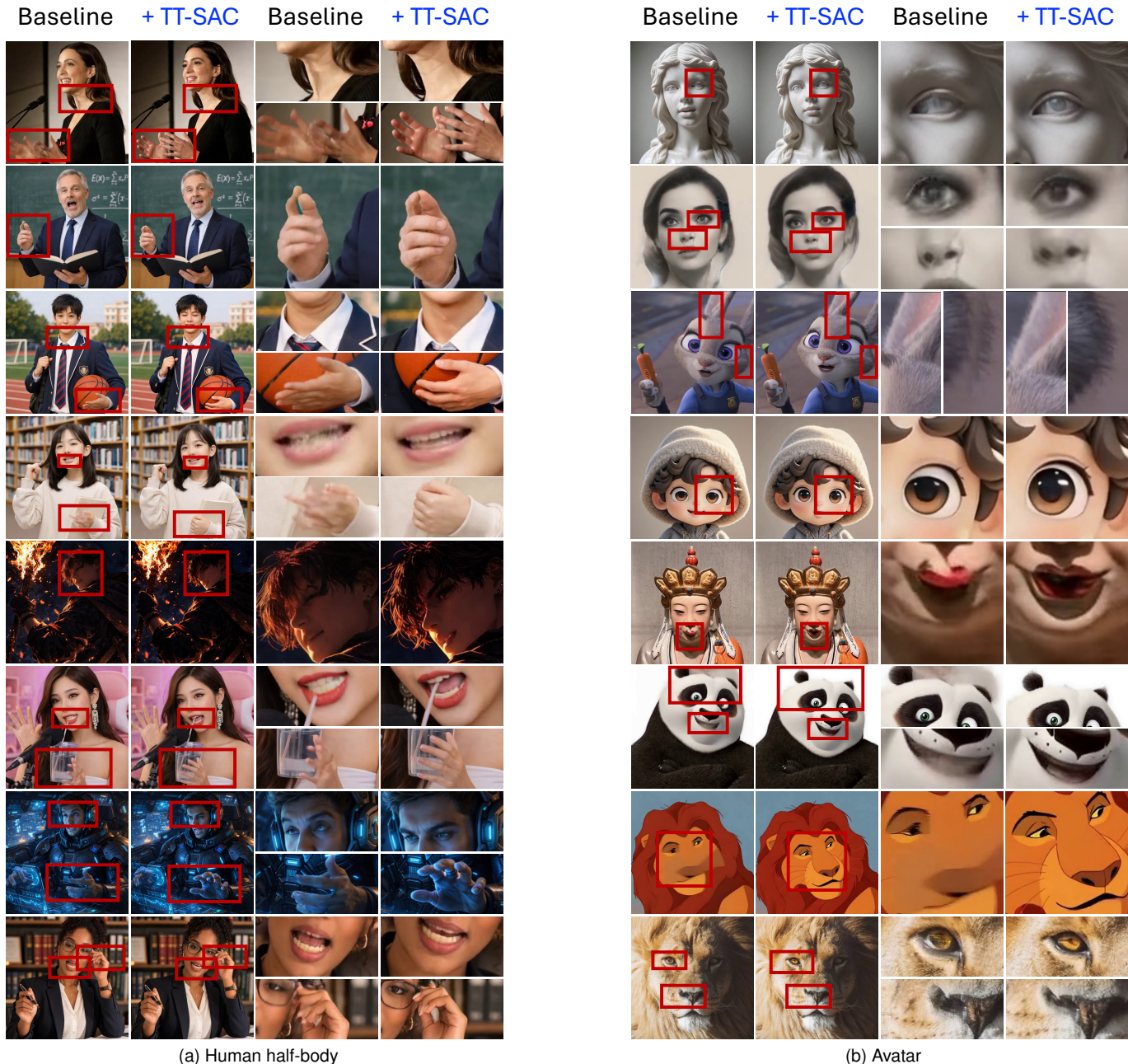


Fig. 5: Generalization to other audio-driven video synthesis tasks in OmniAvatar [49]. Our method improves motion coherence and enhances eye dynamics and fine-grained details in both human half-body generation and avatar animation tasks, demonstrating strong cross-task generalization.

perceptual realism and temporal coherence, leading to better FID/FVD and LPIPS scores for models such as AniTalker and FLOAT. However, improvements in synchronization (Sync-C/Sync-D) and temporal smoothness (Smooth) are not always consistent, and identity-only TT-SAC occasionally achieves slightly stronger alignment metrics. Qualitatively, motion-aware TT-SAC effectively suppresses temporal artifacts commonly observed in baseline models, including sudden facial shifts, frame-to-frame jitter, and structural instability (Fig. 3). These improvements are particularly visible in regions with

large motion dynamics, where identity-only TT-SAC already stabilizes facial appearance while motion-aware TT-SAC further reduces temporal deviations. Identity consistency (CSIM) remains largely preserved relative to baseline, although minor trade-offs can occur for certain model-dataset combinations.

Failure modes and generality. TT-SAC assumes that the initial generation provides sufficiently informative identity cues. If early frames exhibit severe identity degradation, the Monte Carlo estimate may inherit this bias. However, aggregation is performed in encoder feature space rather than pixel

space, and identity-focused encoders tend to suppress transient artifacts, mitigating error amplification. In practice, the first few frames typically retain reliable identity information, making the estimator stable; extreme motion or severely degraded initial outputs may reduce the magnitude of improvement but do not destabilize the process.

Applicability to other video generation tasks. Our method is not tied to a specific talking-head architecture. Since TT-SAC operates purely on the conditioning representation at test time, it can be directly applied to other audio-driven video generation pipelines without modifying model parameters. To demonstrate this generality, we apply TT-SAC to OmniAvatar [49], which supports more challenging synthesis scenarios such as human half-body generation and non-human avatar animation. As shown in Fig. 5, TT-SAC consistently improves temporal stability and visual fidelity in both settings. In half-body synthesis, the method produces more coherent hand and body motion, while in avatar animation it enhances eye dynamics and fine structural details. These results indicate that TT-SAC generalizes beyond face-only talking-head generation and can serve as a test-time conditioning adaptation for diverse audio-driven video synthesis tasks.

V. CONCLUSION

We presented TT-SAC, a conditioning-level test-time adaptation framework for audio-driven talking-head generation. Instead of relying solely on a static reference feature, TT-SAC performs feature aggregation and a single self-consistency update to project the conditioning representation toward a generator-encoder equilibrium. Extensive experiments across multiple datasets and pretrained generators demonstrate consistent improvements in identity preservation, perceptual quality, and video-level realism, with dataset- and model-dependent effects on lip synchronization and temporal smoothness. Motion-aware TT-SAC further enhances stability for several architectures, while preserving alignment and identity in most settings. Our theoretical analysis provides a principled interpretation of TT-SAC through variance reduction and local fixed-point contraction, explaining why small aggregation windows achieve strong empirical performance. Since TT-SAC requires no retraining, architectural modification, or gradient-based adaptation, it serves as a practical and broadly applicable test-time stabilization strategy. We believe this work highlights conditioning self-consistency as a general mechanism for improving stability and coherence in generative video models.

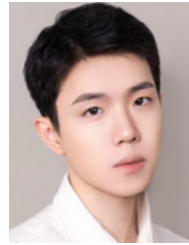
REFERENCES

- [1] A. Siarohin, S. Lathuilière, S. Tulyakov, E. Ricci, and N. Sebe, “First order motion model for image animation,” in *Advances in Neural Information Processing Systems*, 2019, pp. 7135–7145.
- [2] L. Chen, R. K. Maddox, Z. Duan, and C. Xu, “Hierarchical cross-modal talking face generation with dynamic pixel-wise loss,” in *Proceedings of the IEEE/CVF Conference on Computer Vision and Pattern Recognition*, 2019, pp. 7832–7841.
- [3] K. Prajwal, R. Mukhopadhyay, V. P. Nambodiri, and C. Jawahar, “A lip sync expert is all you need for speech to lip generation in the wild,” in *Proceedings of the 28th ACM International Conference on Multimedia*, 2020, pp. 484–492.
- [4] M. Xu, H. Li, Q. Su, H. Shang, L. Zhang, C. Liu, J. Wang, Y. Yao, and S. Zhu, “Hallo: Hierarchical audio-driven visual synthesis for portrait image animation,” *arXiv preprint arXiv:2406.08801*, 2024.
- [5] J. Cui, H. Li, Y. Yao, H. Zhu, H. Shang, K. Cheng, H. Zhou, S. Zhu, and J. Wang, “Hallo2: Long-duration and high-resolution audio-driven portrait image animation,” *arXiv preprint arXiv:2410.07718*, 2024.
- [6] J. Cui, H. Li, Y. Zhan, H. Shang, K. Cheng, Y. Ma, S. Mu, H. Zhou, J. Wang, and S. Zhu, “Hallo3: Highly dynamic and realistic portrait image animation with video diffusion transformer,” in *Proceedings of the Computer Vision and Pattern Recognition Conference*, 2025, pp. 21 086–21 095.
- [7] J. Cui, Y. Chen, M. Xu, H. Shang, Y. Chen, Y. Zhan, Z. Dong, Y. Yao, J. Wang, and S. Zhu, “Hallo4: High-fidelity dynamic portrait animation via direct preference optimization and temporal motion modulation,” *arXiv preprint arXiv:2505.23525*, 2025.
- [8] H. Cheng, L. Lin, C. Liu, P. Xia, P. Hu, J. Ma, J. Du, and J. Pan, “Dawn: Dynamic frame avatar with non-autoregressive diffusion framework for talking head video generation,” *arXiv preprint arXiv:2410.13726*, 2024.
- [9] H. Wei, Z. Yang, and Z. Wang, “Anipportrait: Audio-driven synthesis of photorealistic portrait animation,” *arXiv preprint arXiv:2403.17694*, 2024.
- [10] J. Guo, D. Zhang, X. Liu, Z. Zhong, Y. Zhang, P. Wan, and D. Zhang, “Liveportrait: Efficient portrait animation with stitching and retargeting control,” *arXiv preprint arXiv:2407.03168*, 2024.
- [11] S. Xu, G. Chen, Y.-X. Guo, J. Yang, C. Li, Z. Zhang, Y. Zhang, X. Tong, and B. Guo, “Vasa-1: Lifelike audio-driven talking faces generated in real time,” in *Advances in Neural Information Processing Systems*, 2024, pp. 660–684.
- [12] Z. Zhang, L. Wang, Y. Gao, and Y. Zhang, “Talking-head generation in practice,” in *The Second International Workshop on Transformative Insights in Multifaceted Evaluation at The Web Conference 2026*, 2026. [Online]. Available: <https://openreview.net/forum?id=ns3TgZYQTZ>
- [13] W. Zhang, X. Cun, X. Wang, Y. Zhang, X. Shen, Y. Guo, Y. Shan, and F. Wang, “Sadtalker: Learning realistic 3d motion coefficients for stylized audio-driven single image talking face animation,” in *Proceedings of the IEEE/CVF Conference on Computer Vision and Pattern Recognition*, 2023, pp. 8652–8661.
- [14] T. Liu, F. Chen, S. Fan, C. Du, Q. Chen, X. Chen, and K. Yu, “Anitalker: animate vivid and diverse talking faces through identity-decoupled facial motion encoding,” in *Proceedings of the 32nd ACM International Conference on Multimedia*, 2024, pp. 6696–6705.
- [15] T. Ki, D. Min, and G. Chae, “Float: Generative motion latent flow matching for audio-driven talking portrait,” in *Proceedings of the IEEE/CVF International Conference on Computer Vision*, 2025, pp. 14 699–14 710.
- [16] X. Ji, X. Hu, Z. Xu, J. Zhu, C. Lin, Q. He, J. Zhang, D. Luo, Y. Chen, Q. Lin *et al.*, “Sonic: Shifting focus to global audio perception in portrait animation,” in *Proceedings of the IEEE/CVF Conference on Computer Vision and Pattern Recognition*, 2025, pp. 193–203.
- [17] R. Kumar, J. Sotelo, K. Kumar, A. De Brebisson, and Y. Bengio, “Obamanet: Photo-realistic lip-sync from text,” *arXiv preprint arXiv:1801.01442*, 2017.
- [18] H. Kim, P. Garrido, A. Tewari, W. Xu, J. Thies, M. Niessner, P. Pérez, C. Richardt, M. Zollhöfer, and C. Theobalt, “Deep video portraits,” *ACM transactions on graphics (TOG)*, vol. 37, no. 4, pp. 1–14, 2018.
- [19] S. Suwajanakorn, S. M. Seitz, and I. Kemelmacher-Shlizerman, “Synthesizing obama: learning lip sync from audio,” *ACM Transactions on Graphics (ToG)*, vol. 36, no. 4, pp. 1–13, 2017.
- [20] T. Karras, T. Aila, S. Laine, A. Herva, and J. Lehtinen, “Audio-driven facial animation by joint end-to-end learning of pose and emotion,” *ACM Transactions on Graphics (ToG)*, vol. 36, no. 4, pp. 1–12, 2017.
- [21] J. S. Chung and A. Zisserman, “Out of time: automated lip sync in the wild,” in *Asian Conference on Computer Vision*, 2016, pp. 251–263.
- [22] S. A. Jalalifar, H. Hasani, and H. Aghajan, “Speech-driven facial reenactment using conditional generative adversarial networks,” *arXiv preprint arXiv:1803.07461*, 2018.
- [23] R. Yi, Z. Ye, J. Zhang, H. Bao, and Y.-J. Liu, “Audio-driven talking face video generation with learning-based personalized head pose,” *arXiv preprint arXiv:2002.10137*, 2020.
- [24] J. Thies, M. Zollhofer, M. Stamminger, C. Theobalt, and M. Nießner, “Face2face: Real-time face capture and reenactment of rgb videos,” in *Proceedings of the IEEE/CVF Conference on Computer Vision and Pattern Recognition*, 2016, pp. 2387–2395.
- [25] T.-C. Wang, A. Mallya, and M.-Y. Liu, “One-shot free-view neural talking-head synthesis for video conferencing,” in *Proceedings of the IEEE/CVF Conference on Computer Vision and Pattern Recognition*, 2021, pp. 10 039–10 049.
- [26] Y. Ma, S. Zhang, J. Wang, X. Wang, Y. Zhang, and Z. Deng, “Dreamtalk: When emotional talking head generation meets diffusion probabilistic models,” *arXiv preprint arXiv:2312.09767*, 2023.

- [27] M. Wang, Q. Wang, F. Jiang, Y. Fan, Y. Zhang, Y. Qi, K. Zhao, and M. Xu, "Fantasytalking: Realistic talking portrait generation via coherent motion synthesis," in *Proceedings of the 33rd ACM International Conference on Multimedia*, 2025, pp. 9891–9900.
- [28] Z. Kong, F. Gao, Y. Zhang, Z. Kang, X. Wei, X. Cai, G. Chen, and W. Luo, "Let them talk: Audio-driven multi-person conversational video generation," *arXiv preprint arXiv:2505.22647*, 2025.
- [29] X. Ma, J. Cai, Y. Guan, S. Huang, Q. Zhang, and S. Zhang, "Playmate: Flexible control of portrait animation via 3d-implicit space guided diffusion," *arXiv preprint arXiv:2502.07203*, 2025.
- [30] Z. Chen, J. Cao, Z. Chen, Y. Li, and C. Ma, "Echomimic: Lifelike audio-driven portrait animations through editable landmark conditions," in *Proceedings of the AAAI Conference on Artificial Intelligence*, vol. 39, no. 3, 2025, pp. 2403–2410.
- [31] N. Drobyshev, J. Chelishchev, T. Khakhulin, A. Ivakhnenko, V. Lempitsky, and E. Zakharov, "Megaportraits: One-shot megapixel neural head avatars," in *Proceedings of the 30th ACM International Conference on Multimedia*, 2022, pp. 2663–2671.
- [32] W. Tan, C. Lin, C. Xu, F. Xu, X. Hu, X. Ji, J. Zhu, C. Wang, and Y. Fu, "Disentangle identity, cooperate emotion: Correlation-aware emotional talking portrait generation," in *Proceedings of the 33rd ACM International Conference on Multimedia*, 2025, pp. 9987–9995.
- [33] D. Ding, L. Wang, L. Zhu, T. Gedeon, and P. Koniusz, "Learnable expansion of graph operators for multi-modal feature fusion," in *The Thirteenth International Conference on Learning Representations*, 2025. [Online]. Available: <https://openreview.net/forum?id=SMZqIOSdIN>
- [34] Z. Liu, X. Liu, S. Chen, J. Liu, L. Wang, and C. Bi, "Multimodal fusion for talking face generation utilizing speech-related facial action units," *ACM Transactions on Multimedia Computing, Communications and Applications*, vol. 20, no. 9, pp. 1–24, 2024.
- [35] J. Guan, Z. Zhang, H. Zhou, T. Hu, K. Wang, D. He, H. Feng, J. Liu, E. Ding, Z. Liu *et al.*, "Stylesync: High-fidelity generalized and personalized lip sync in style-based generator," in *Proceedings of the IEEE/CVF Conference on Computer Vision and Pattern Recognition*, 2023, pp. 1505–1515.
- [36] J. Ho, A. Jain, and P. Abbeel, "Denoising diffusion probabilistic models," in *Advances in Neural Information Processing Systems*, 2020, pp. 6840–6851.
- [37] J. Song, C. Meng, and S. Ermon, "Denoising diffusion implicit models," *arXiv preprint arXiv:2010.02502*, 2020.
- [38] Y. Lipman, R. T. Chen, H. Ben-Hamu, M. Nickel, and M. Le, "Flow matching for generative modeling," *arXiv preprint arXiv:2210.02747*, 2022.
- [39] C. Lu, Y. Zhou, F. Bao, J. Chen, C. Li, and J. Zhu, "Dpm-solver: A fast ode solver for diffusion probabilistic model sampling in around 10 steps," in *Advances in Neural Information Processing Systems*, 2022, pp. 5775–5787.
- [40] N. Metropolis and S. Ulam, "The monte carlo method," *Journal of the American statistical association*, vol. 44, no. 247, pp. 335–341, 1949.
- [41] S. Banach, "Sur les opérations dans les ensembles abstraits et leur application aux équations intégrales," *Fundamenta mathematicae*, vol. 3, no. 1, pp. 133–181, 1922.
- [42] S. R. Livingstone and F. A. Russo, "The ryerson audio-visual database of emotional speech and song (ravdess): A dynamic, multimodal set of facial and vocal expressions in north american english," *PLoS one*, vol. 13, no. 5, p. e0196391, 2018.
- [43] H. Zhu, W. Wu, W. Zhu, L. Jiang, S. Tang, L. Zhang, Z. Liu, and C. C. Loy, "Celebv-hq: A large-scale video facial attributes dataset," in *European Conference on Computer Vision*, 2022, pp. 650–667.
- [44] X. Cao, G. Wang, S. Shi, J. Zhao, Y. Yao, J. Fei, and M. Gao, "Joyvasa: portrait and animal image animation with diffusion-based audio-driven facial dynamics and head motion generation," *arXiv preprint arXiv:2411.09209*, 2024.
- [45] S. Jayasumana, S. Ramalingam, A. Veit, D. Glasner, A. Chakrabarti, and S. Kumar, "Rethinking fid: Towards a better evaluation metric for image generation," in *Proceedings of the IEEE/CVF Conference on Computer Vision and Pattern Recognition*, 2024, pp. 9307–9315.
- [46] T. Unterthiner, S. Van Steenkiste, K. Kurach, R. Marinier, M. Michalski, and S. Gelly, "Towards accurate generative models of video: A new metric & challenges," *arXiv preprint arXiv:1812.01717*, 2018.
- [47] J. Deng, J. Guo, N. Xue, and S. Zafeiriou, "Arcface: Additive angular margin loss for deep face recognition," in *Proceedings of the IEEE/CVF Conference on Computer Vision and Pattern Recognition*, 2019, pp. 4690–4699.
- [48] R. Zhang, P. Isola, A. A. Efros, E. Shechtman, and O. Wang, "The unreasonable effectiveness of deep features as a perceptual metric,"

in *Proceedings of the IEEE/CVF Conference on Computer Vision and Pattern Recognition*, 2018, pp. 586–595.

- [49] Q. Gan, R. Yang, J. Zhu, S. Xue, and S. Hoi, "Omniavatar: Efficient audio-driven avatar video generation with adaptive body animation," *arXiv preprint arXiv:2506.18866*, 2025.



Zhicheng Zhang is a Ph.D. student at the University of New South Wales (UNSW), Australia, supervised by Dr. Yu Zhang (2024-present). He received his M.S. from The University of Queensland, Australia (2022–2023). He is currently a visiting scholar at the ARC Research Hub hosted by Griffith University, under the supervision of Dr. Lei Wang and Prof. Yongsheng Gao. He also serves as the workshop coordinator for the TIME 2026 workshop, organized as part of The Web Conference 2026 (WWW 2026). His research interests include talking-head generation, temporal modeling, and computer vision.



Lei Wang received his M.E. in Software Engineering from the University of Western Australia (UWA) in 2018 and his Ph.D. in Engineering and Computer Science from the Australian National University (ANU) in 2023. He is a Research Fellow in the School of Electrical and Electronic Engineering at Griffith University and a Visiting Scientist with Data61/CSIRO. He leads the Temporal Intelligence and Motion Extraction (TIME) Lab at Griffith University. He previously held research positions at ANU, UWA, and Data61/CSIRO. His research

focuses on motion-, data-, and model-centric approaches to video action recognition and anomaly detection. He has authored numerous first-author papers in top-tier venues, including CVPR, ICCV, ECCV, ACM Multimedia, NeurIPS, ICLR, ICML, AAAI, TPAMI, IJCV, and TIP, and received the Sang Uk Lee Best Student Paper Award at ACCV 2022. He serves as an Area Chair for ACM Multimedia 2024–2025, ICASSP 2025, and ICPR 2024, and was recognized as an Outstanding Area Chair at ACM Multimedia 2024.



Yu Zhang is a Lecturer in Data Science at the School of Business, UNSW. His research focuses on machine learning for information and knowledge management, graph representation learning and heterogeneous network analysis, text and data mining for asset management, AI-driven industrial systems, sustainable logistics, and net-zero energy solutions. He has led and contributed to multiple government- and industry-funded projects on trustworthy AI for battery health monitoring, AI-enabled defense logistics, cyber threat intelligence, and hybrid energy systems for net-zero buildings. His work has been published in leading journals and conferences, including Information Processing & Management, Journal of Informetrics, AAAI, CIKM, and PAKDD. He has received several Best/Excellent Paper Awards, including ADMA 2024, ICEBE 2024, and VICFCNT 2020.



Yongsheng Gao received the BSc and MSc degrees in Electronic Engineering from Zhejiang University, China, in 1985 and 1988, respectively, and the PhD degree in Computer Engineering from Nanyang Technological University, Singapore. He is currently a Professor at the School of Engineering and Built Environment, Griffith University, and Director of the ARC Research Hub for Driving Farming Productivity and Disease Prevention, Australia. He was previously the Leader of the Biosecurity Group at the Queensland Research Laboratory, National ICT Australia (ARC Centre of Excellence), a consultant at Panasonic Singapore Laboratories, and an Assistant Professor at Nanyang Technological University. His research interests include smart farming, machine vision for agriculture, biosecurity, face recognition, biometrics, image retrieval, computer vision, pattern recognition, environmental informatics, and medical imaging. He is a recipient of the 2025 ARC Industry Laureate Fellow.